



## Effects of cryoprotectant addition and washout methods on the viability of precision-cut liver slices<sup>☆</sup>

Na Guan<sup>a</sup>, Sylvia A. Blomsma<sup>a</sup>, Paul M. van Midwoud<sup>a,b</sup>, Gregory M. Fahy<sup>c</sup>, Geny M.M. Groothuis<sup>a</sup>, Inge A.M. de Graaf<sup>a,\*</sup>

<sup>a</sup> Division of Pharmacokinetics, Toxicology and Targeting, Department of Pharmacy, University of Groningen, The Netherlands

<sup>b</sup> Laboratory of Food & Nutrition Toxicology, ETH Zurich, Switzerland

<sup>c</sup> Twenty-First Century Medicine, Fontana, CA, USA

### ARTICLE INFO

#### Article history:

Received 13 February 2012

Accepted 14 May 2012

Available online 18 June 2012

#### Keywords:

Cryoprotectants

Step-wise cryoprotectant loading

Gradient-wise cryoprotectant loading

Chemical toxicity

Cryoprotectant toxicity

Tissue banking

Cryopreservation

Ice-free cryopreservation

Vitrification

Osmosis

### ABSTRACT

Successful vitrification of organ slices is hampered by both osmotic stress and chemical toxicity of cryoprotective agents (CPAs). In the present study, we focused on the effect of osmotic stress on the viability of precision-cut liver slices (PCLS) by comparing different CPA solutions and different methods of loading and unloading the slices with the CPAs. For this purpose, we developed a gradient method to load and unload CPAs with the intention of minimizing sudden changes in osmolarity and thereby avoiding osmotic stress in the slices in comparison with the commonly used step-wise loading/unloading approach. With this gradient method, the CPA solution was introduced at a constant rate into a specially designed mixing chamber containing the slices. We showed that immediate mixing of the infused CPA and the chamber constituents occurred, which enabled us to control the CPA concentration to which PCLS were exposed as a function of time.

With this method, CPA concentration versus time profiles were varied using various commercially available CPA mixtures [VMP, VM3, M22, and modified M22 (mM22)]. The viability of PCLS was determined after CPA loading and unloading and subsequent incubation during 3 h at 37 °C. Despite the reduction of osmotic stress, the viability of slices did not improve with gradual loading and unloading and remained considerably lower than that of untreated slices. The toxicity of the three CPA solutions did not correlate with either their potential osmotic effects or their total concentrations, and did not change strongly with exposure time in 100% CPA. The most likely explanation for these observations is that PCLS are not very sensitive to osmotic changes of the magnitude imposed in our study, and chemical toxicity of the CPA solutions is the main barrier to be overcome. The chemical toxicity of the CPAs used in this study probably originates from a source other than the total concentration of the solutions. The presented gradient method using the specially designed chamber is more time and cost effective than the step-wise method and can be universally applied to efficiently evaluate different CPA solutions.

© 2012 Elsevier Inc. All rights reserved.

### Introduction

Precision-cut liver slices (PCLS) from various species have been widely used to study the pathology of diseases as well as the

*Abbreviations:* PCLS, precision-cut liver slices; CPA, cryoprotective agent; Me<sub>2</sub>SO, dimethylsulfoxide; WME, William's medium E; UW, University of Wisconsin medium.

<sup>☆</sup> *Statement of funding:* This research is supported by the Dutch Technology Foundation STW, which is the applied science division of NWO and the Technology Program of the Ministry of Economic Affairs, and by N.V. Organon, Inc. (now MSD Oss B.V.) and 21st Century Medicine, Inc.

\* Corresponding author. Address: Department of Pharmacokinetics, Toxicology and Targeting, Groningen Research Institute for Pharmacy, University of Groningen, Antonius Deusinglaan 1, 9713 AV Groningen, The Netherlands. Fax: +31 50 3633247.

E-mail address: [I.A.M.de.Graaf@rug.nl](mailto:I.A.M.de.Graaf@rug.nl) (I.A.M. de Graaf).

absorption, distribution, metabolism, elimination and toxicity (ADME-Tox) of drugs [1,2,28,29,32,35,36]. Successful cryopreservation of PCLS would allow the creation of a tissue bank with PCLS from various species, which would be particularly valuable for enabling the use of human PCLS because of the scarcity of human material. The availability of a tissue bank with human PCLS would greatly facilitate the research and application of human PCLS and reduce the use of laboratory animals. Nowadays in the pharmaceutical industry, human hepatocytes are preferred for ADME-Tox studies over PCLS because cryopreserved human hepatocytes can be obtained commercially, despite some evident disadvantages of the hepatocytes. Cryopreservation of PCLS by rapid or slow freezing in the presence of DMSO was published before, but the resultant viability was not satisfactory for all species (unpublished observations for human and dog slices) or after incubations longer

than 3–6 h after retrieval from cryopreservation [21,22]. To overcome such problems, vitrification, by which an aqueous solution turns to a glass without ice crystal formation, was suggested as a better alternative method for cryopreservation [7,12,15].

Vitrification has been successfully used for the cryopreservation of different cell types [8], embryos [30,38], tissues [5,27] and organs [13,23] and is considered to be the most promising starting point for the cryopreservation of PCLS. Although there have been some successes in the vitrification of cells with little or no cryoprotectant [20], this is only possible for either extremely small systems and/or for systems with very low water content, so in most cases highly concentrated cryoprotectant (CPA) solutions are required to prevent ice formation [15].

During the loading and unloading of CPAs, living organisms or tissues can suffer from damage induced by both chemical toxicity and osmotic stress caused by these CPAs. [17]. The chemical toxicity of CPAs is considered to be “a fundamental limiting factor for the successful cryopreservation of living systems by both freezing and vitrification” [10], but Fahy reported that the overall chemical toxicity of a CPA solution can be reduced by mixing different CPAs with different mechanisms of toxicity. Moreover he suggested that in some cases the toxicity of one agent can actually be blocked by the presence of a second agent in the solution such that vitrification can be achieved with little or no toxicity from the CPA solution [10,14,15]. Nowadays solutions based on these principles such as VM3, VMP, and M22 are commercially available and have been successfully used for the vitrification of rat [7] and rabbit [15] kidney slices.

Osmotic damage induced during CPA loading and unloading is caused by shrinkage or swelling of cells in response to the imposed osmotic gradient beyond the tolerance limits of the cells in question. Osmotic damage may at least partly be prevented by loading/unloading the CPA solutions using concentration steps of limited size, exposing cells [25] or tissues [37] to a series of CPA solutions from low to high concentrations during the CPA addition phase and from high to low concentrations during the CPA wash-out phase. This step-wise approach aims to allow the cells or tissues enough time to recover approximately their normal volumes after each change in osmolarity before the next change is introduced. In addition, it was shown that osmotic stress can be reduced during unloading by addition of, for example, the non-penetrating sugars sucrose or trehalose to reduce osmotic water uptake [5,7,26].

In principle, exposing cells to a continuous concentration gradient should be less dangerous than exposing them to step changes in CPA concentration, provided the imposed rates of change of concentration are compatible with the cells' permeability to CPA. Therefore, we examined a semi-automated gradient method for gradual loading and unloading of precision-cut rat liver slices with CPAs. Using this gradient method, step-wise osmotic shifts were avoided so that osmotic stress experienced by liver slices was reduced. This gradient method for CPA loading/unloading was applied to different CPA solutions (M22 [15], VM3 [21] and mM22 (a slightly modified version of M22)). The susceptibility of PCLS to osmotic stress was evaluated by determining their viability after CPA loading and unloading by various gradient profiles and step-wise methods using ATP content and morphological appearance as end-points.

## Materials and methods

### Chemical and reagents

Gentamicin and William's medium E (WME) supplemented with Glutamax I were purchased from Gibco (Paisley, UK). D-glu-

cose monohydrate was obtained from Sigma–Aldrich (St Louis, MO, USA). University of Wisconsin solution (UW) was obtained from DuPont Pharmaceuticals, Waukegan, IL, USA. The constituents of VM3, VMP (VM3 without PVP), M22 and modified M22 (M22 without 2% *N*-methylformamide) are listed in Table 1 and were a gift from 21st Century Medicine, Fontana, California, USA, which is the patent holder for these solutions. The ATP bioluminescence assay kit was purchased from Roche (Mannheim, Germany). D-(+)-Trehalose dehydrate and Me<sub>2</sub>SO (>99.9% pure) were from Sigma–Aldrich Chemical Co. (St. Louis, MO, USA). All other reagents and materials used were of the highest purity and were commercially available.

### Preparation of CPA working solutions

100% working solutions for VMP, VM3, M22 and mM22 were prepared by adding pre-mixed concentrated CPA solutions as obtained from 21st Century Medicine to a concentrated version of the carrier solution LM5. The composition of LM5, as indicated in Table 1, was as in [15], but calcium and magnesium were omitted. The concentration of LM5 was the same in all the 100% working CPA solutions regardless of the amount of cryoprotectant present in the solution. The final concentrations of all solution constituents used for this study were as advised by the manufacturer and are indicated in Table 1. For the step-wise method, 100% CPA working solutions were diluted using LM5 to create the loading step solutions or using LM5 containing 300 mM trehalose to create the unloading step solutions.

### Animals and preparation of liver slices

Male Wistar rats (HsdCpb:WU) (300–350 g) obtained from Harlan (Horst, The Netherlands) were used for all experiments. The rats were maintained under a 12-h light/dark cycle in a temperature- and humidity-controlled room with food (Harlan chow No. 2018, Horst, The Netherlands) and tap water *ad libitum*. The animal experimental protocol was approved by the Animal Ethical Committee of the University of Groningen.

PCLS were prepared as described previously [7]. Briefly, the liver was excised after anesthetizing the rats with isoflurane/oxygen. Subsequently, cylindrical cores of liver tissue with a diameter of 5 mm were made by utilizing a hollow drill bit. Cores were placed in a Krumdieck tissue slicer (Alabama R&D, Munford, AL, USA) containing ice-cold Krebs–Henseleit saturated with a mixture of 95% oxygen and 5% CO<sub>2</sub>. PCLS were produced with a thickness of 250 μm and a wet weight of approximately 5 mg.

**Table 1**

Composition of 100% working solutions of VMP [7], VM3 [7,14], M22 [15] and mM22.

	VMP	VM3	M22	mM22
Me <sub>2</sub> SO (g/L)	223.1	223.1	223.1	223.1
Formamide (g/L)	128.6	128.6	128.6	128.6
Ethylene glycol (g/L)	168.4	168.4	168.4	168.4
<i>N</i> -Methylformamide (g/L)	–	–	30	10
3-Methoxy,1,2-propanediol (g/L)	–	–	40	40
PVP K12 (g/L)	–	70	28	28
Supercool X-1000 <sup>a</sup> (g/L)	10	10	10	10
Supercool Z-1000 <sup>a</sup> (g/L)	10	10	20	20
5 × LM5 (mL/L) <sup>a</sup>	200	200	200	200
Total CPA molarity	8.4	8.4	9.3	9.0

The composition of the 1X LM5 carrier solution is 90 mM glucose, 45 mM mannitol, 45 mM lactose, 28.2 mM KCl, 7.2 mM K<sub>2</sub>HPO<sub>4</sub>, 5 mM reduced glutathione, 1 mM adenine HCl, 10 mM NaHCO<sub>3</sub> [15].

<sup>a</sup> Ice blocker.

*Design and fabrication of equilibration chamber*

A Computer Numerical Controlled (CNC)-milled equilibration chamber was produced in-house from polycarbonate (ERIKS Kunststoffen, Leek, The Netherlands). The device as depicted in Fig. 1 contains two flow-through chambers, and in both of them a histology cassette (Histosette I, Simport Ltd., Canada) containing PCLS is placed. The outer dimensions are 100 × 100 × 20 mm (L × W × H), and the dimension of one chamber is approximately 42 × 28 × 13 mm (L × W × H). The inlet widens up to ensure an even and gradual flow of liquid into the histology cassette, to induce immediate mixing of the chamber contents with the inflowing medium, thereby resulting in a concentration gradient in the chamber. Simulations with Comsol Multiphysics (Comsol, UK) confirmed the hypothesis that a uniform solvent velocity distribution is obtained across the chamber, as can be seen in Fig. 1c. A flat polycarbonate cover lid was used to close the device with finger-tight screws. Rubber O-rings surrounded the two chambers (Fig. 1b) to ensure a leak-tight connection.

*Setup of the semi-automated gradient method for CPA loading and unloading*

Fig. 2 illustrates the instrumental setup of the gradient method for CPA loading and unloading. The system consists of the specially designed mixing chamber (described in Fig. 1) that is interconnected between a plunger pump [Hewlett Packard 1100 Series HPLC quaternary pump (Palo Alto, CA)] and a waste depot via PEEK tubing (1/16" OD × 0.50 mm ID, DaVinci Europe, Rotterdam, The

Netherlands). The volume of the chamber is about 15 cm<sup>3</sup> in which 10–20 organ slices were placed inside a cassette that is normally used for paraffin embedding of tissue for histology (Histosette I, Simport Ltd., Canada). The cassette prevented the slices from flowing to the outlet of the chamber.

At the beginning of the process, the chamber was filled with the carrier solution LM5 and the cassettes with slices were put into the chamber. Then the chamber was closed with finger-tight screws. Subsequently, different CPA solutions were pumped into the chamber and thereby gradually replaced the LM5. Several gradient methods for CPA loading and unloading were evaluated, and the detailed protocols are described below and in Figs. 3–5. The infused solution was mixed with the LM5 solution in the chamber by diffusion and convection at least partly as a result of the special shape of the chamber, thereby gradually increasing the CPA concentration. After the CPA loading step was completed, the slices were removed from the chamber, and were subsequently incubated with 100% CPA working solution for an additional 5 or 15 min.

The flow rate through the chamber was set at 1.0 or 1.3 ml/min. The impact of the shear stress induced by the flow of medium on the viability of PCLS was studied by introducing UW instead of CPA to the PCLS within the chamber by the pump at a flow rate of 1.3 ml/min for 105 min, whereas PCLS submerged into ice-cold UW during the whole procedure served as controls.

During the CPA unloading step, the slices loaded with 100% CPA were placed in the chamber in 100% CPA working solution, and LM5 with 300 mM trehalose was introduced into the chamber for 30 min at a flow rate of 1.3 ml/min. Then the slices were removed from the chamber and an additional washing step with LM5 with

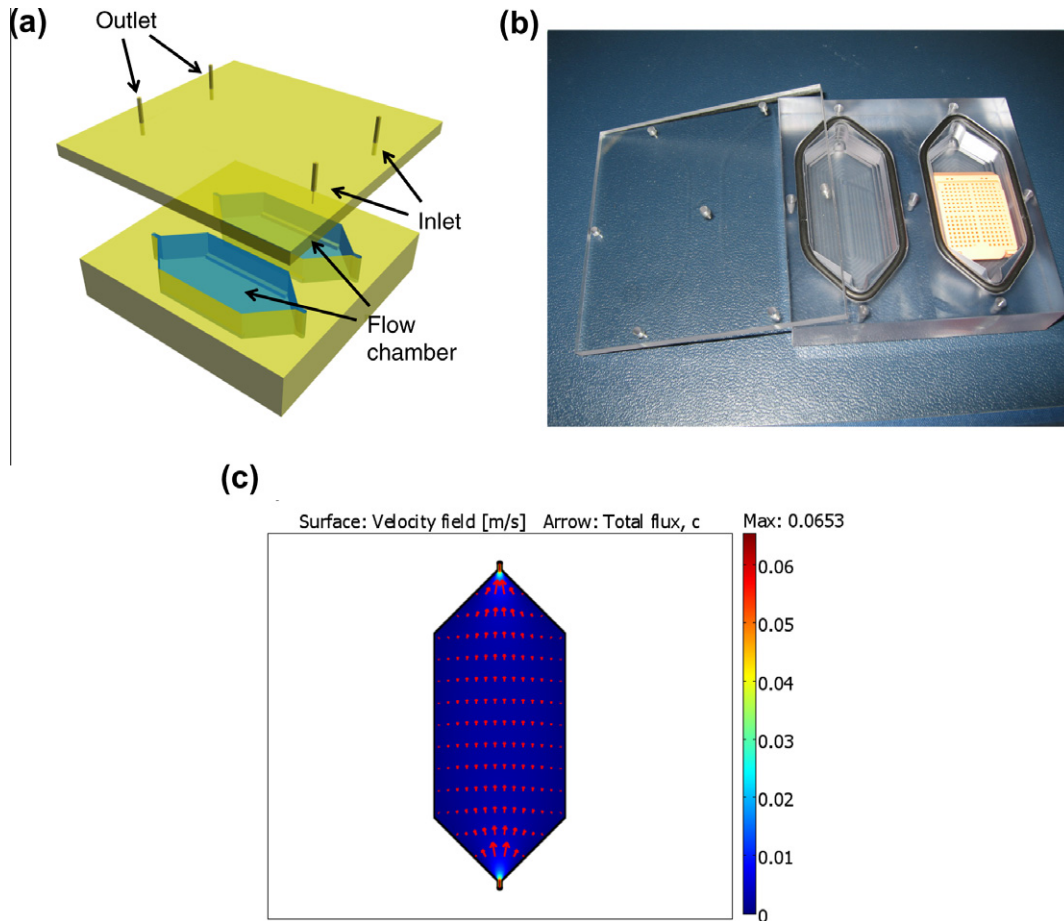


**Fig. 1.** (a) Schematic illustration of the chamber for gradient loading and unloading of CPAs. The dimensions of one sub-chamber are 42 × 28 × 13 mm (L × W × H). (b) Picture of the chamber with a histology cassette in one of the sub-chambers. Slices are placed into the histology cassette, which is placed into each of the sub-chambers. (c) A Comsol Multiphysics simulation of the flow profile in one sub-chamber. The length of the red arrows indicates the local flow rate.

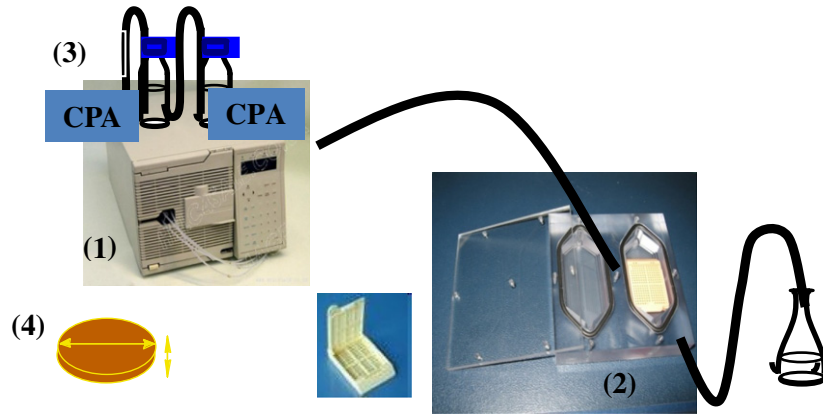


**Fig. 2.** Schematic overview of the semi-automated method for CPA loading and unloading for PCLS. The system consists of a plunger pump (1), an equilibration chamber with histology cassette (2), CPA solution (3). (4) Schematic representation of a liver slice with a diameter of 5 mm and a thickness of 250  $\mu\text{m}$ .

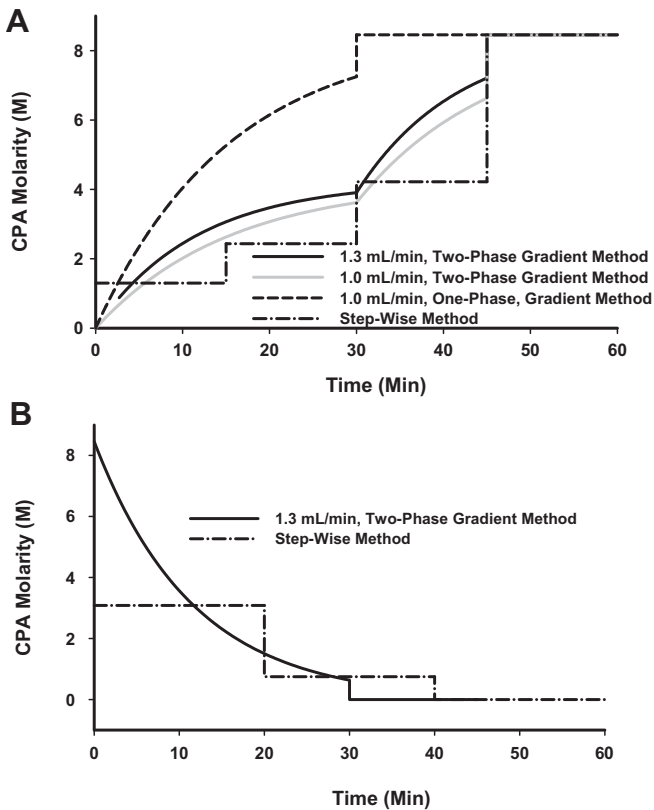


**Fig. 3.** Schematic diagrams of different loading/unloading profiles for VM3 for PCLS. A. the profiles of concentration vs time for VM3 loading. For the two-phase gradient method 50% VMP solution was pumped into the chamber at a rate of either 1.0 or 1.3 ml/min for 30 min, followed by 100% VM3 working solution for 15 min. For the one-phase gradient method, 100% VM3 was pumped into the chamber over 30 min at the flow rate of 1.0 ml/min, and slices were removed from the chamber and immersed in 100% VM3 for an additional 15 min. For the stepwise method, slices were sequentially treated with 16% VMP (15 min), 30% VMP (15 min), 52% VMP (15 min) and 100% VM3 (15 min). B. Concentration–time profiles for VM3 unloading. For both one-phase and two-phase methods, LM5 with 300 mM trehalose was pumped into the chamber over 30 min at the same flow rate as for the loading process. After that, slices were removed from the chamber and were immersed in LM5 with 300 mM trehalose for an additional 15 min. For stepwise unloading, slices were sequentially incubated with 52% VMP (10 min), 30% VMP (10 min), 16% VMP (10 min) and LM5 (10 min); 300 mM trehalose was present in all of these unloading steps.

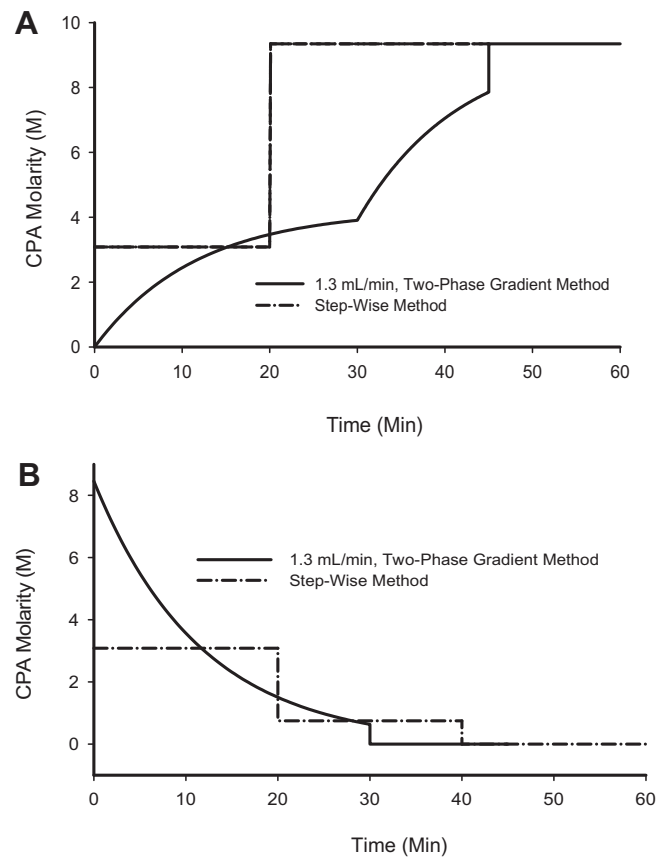


**Fig. 4.** Schematic diagrams of different loading/unloading profiles for M22 for PCLS: A. the profiles of concentration vs time for M22 loading; for the two-phase gradient method, 50% VMP solution was pumped into the chamber at a rate of 1.3 ml/min over 30 min, followed by 100% M22 working solution for 15 min. Thereafter, slices were removed from the chamber and incubated with 100% M22 for an additional 15 min. For the stepwise method, slices were exposed first to 33% M22 (20 min) and then directly to 100% M22 (14 min), followed by an additional 100% M22 exposure step of 5 or 15 min. B. Concentration–time profiles for M22 unloading. For the two-phase gradient method, LM5 with 300 mM trehalose was pumped into the chamber for 30 min at 1.3 ml/min. After that, slices were removed from the chamber and were incubated with LM5 containing 300 mM trehalose for an additional 15 min. For stepwise unloading, slices were sequentially incubated in 33% M22 (20 min), 8% M22 (20 min), and LM5 (20 min), with 300 mM trehalose in all of these unloading steps.

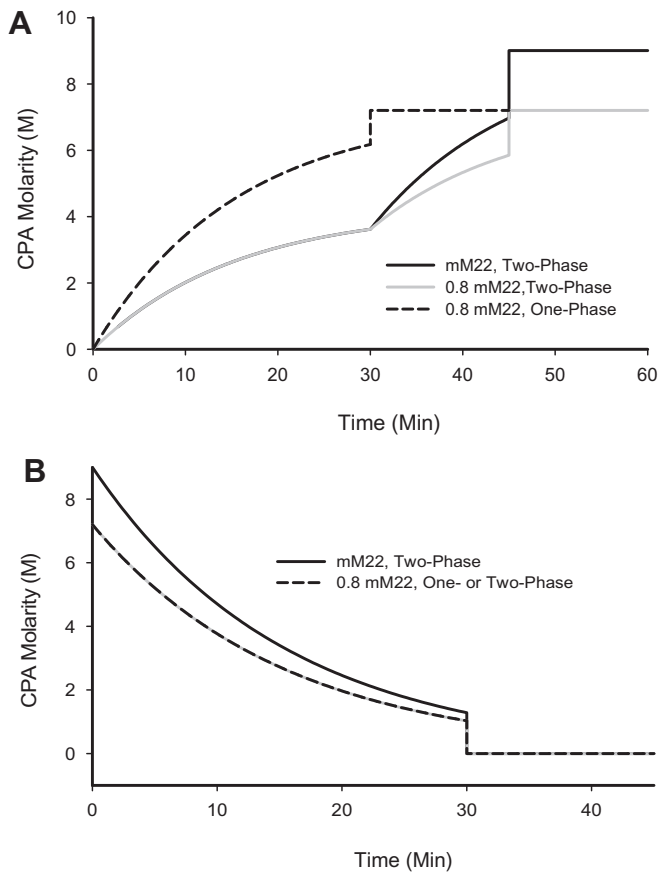


**Fig. 5.** Schematic diagrams of different loading/unloading profiles for mM22 in PCLS. A. Concentration–time profile for mM22 loading. For the two-phase gradient method, 50% VMP was pumped into the chamber at a rate of 1.0 ml/min for 30 min, followed by 100% mM22 or 80% mM22 for an additional 15 min. For the one-phase gradient method, mM22 was pumped into the chamber for 30 min at 1.0 ml/min. Thereafter, slices were removed from the chamber and incubated with 80% or 100% mM22 for an additional 5 or 15 min. B. Concentration–time profiles for CPA unloading. For both one-phase and two-phase methods, LM5 with 300 mM trehalose was pumped into the chamber over 30 min at 1.0 ml/min. After that, slices were removed from the chamber and were incubated with LM5 with 300 mM trehalose for an additional 15 min. Note that the two unloading curves for 0.8 mM22, two- and one-phase methods are superimposed.

300 mM trehalose was applied for 15 min to complete removal of the CPA from the PCLS.

During the whole experiment, the CPA solutions and chamber were immersed in ice to reduce the chemical toxicity of the CPAs. PCLS that did not undergo loading and unloading with CPAs served as controls. Some slices were transferred directly from the 100% VM3 working solution into LM5, and kept in LM5 for 10 min. Since we expected that this sudden change in osmolarity would induce severe damage, these slices served as a negative control for the ATP assay.

For the gradient method, the total amount of time required for the loading and unloading of the CPAs was kept the same as for the step-wise method (see below).

#### Calculation of CPA concentration during loading/unloading with the gradient method

The concentration of CPA in the chamber ( $C_c$ ) at a certain time point ( $t$ ) was calculated assuming immediate mixture in the chamber by using the following equation for a perfectly stirred reactor with continuous flow,

$$C_c = C_{c,0} + C_p(1 - e^{-Rt/V_c})$$

where  $C_p$  represents the concentration of CPA in the perfusion solution,  $R$  represents the perfusion rate of the CPA solution (1.0–1.3 ml/min) and  $V_c$  is the volume of the chamber and tubing (15.4 mL). The perfusion rate was chosen in such a way that at the end of loading and unloading the concentration was >80% (loading) and <10% (unloading) of the 100% working solution. The total exposure time of approximately 40 min was based on the intention to keep the exposure time during VM3 loading and unloading the same for both the gradient method and the stepwise method.

Using this equation, the CPA concentrations in the chamber at each time during loading and unloading for the different one and two phase gradient profiles were calculated for each CPA and plotted in Fig. 3 (VM3), Fig. 4 (M22), and Fig. 5 (mM22). The fluid diffusion and convection within the chamber was checked by addition of a red dye, sulforhodamine (SRB) (Eastman Kodak Co., Rochester, NY USA) to the CPA during the loading step. The VM3 solution containing SRB was introduced into the chamber according to the method described in Fig. 2 to mimic the two-phase gradient step with the exception that 50% VM3 instead of 50% VMP was used. The 0.2 mL outflow was collected every 3 min until the end of the loading step (16 points). Since SRB was dissolved in VM3 the concentration of SRB was directly indicative for the concentration of VM3. The standard curve was prepared by serial dilution of a stock solution of 0.18 mg/mL in 100% VM3 working solution, with LM5. Using the standard curve, the concentration VM3 in the outflow medium was calculated by making use of the absorption at 510 nm by SRB and was then expressed as % of the absorbance of 0.18 mg/mL SRB in the 100% of VM3 working solution. The measured concentration of VM3 was compared to the concentrations calculated using the equation described above.

#### Step-wise method for CPA loading and unloading

For the step-wise method, about 10–20 tissue slices were placed into a 100 ml beaker, which was placed in a container filled with ice, and exposed to a series of CPA in increasing concentrations (from 0–100% working solution) for the CPA loading steps and then decreasing concentrations for CPA unloading (from 100% to 0% working solution). The incubation time in 100% working solution was varied from 5–30 min, as with the gradient method. Throughout the process, the beakers were placed on ice and gently shaken. The steps chosen were based on methods developed for rabbit kidney and liver slices at 21st Century Medicine and are described in the legends of Fig. 3 for VM3 [5,7] and of Fig. 4 for M22. Trehalose was included in all the unloading solutions at a final concentration of 300 mM. All dilutions of the 100% CPA working solutions were prepared using the carrier solution LM5 [15].

#### Incubation and viability testing

After CPA loading and unloading, slices were incubated in 12-well plates (Greiner Bio-One, the Netherlands) under humidified carbogen atmosphere (95% O<sub>2</sub>, 5% CO<sub>2</sub>) in WME, supplemented with 25 mM D-glucose and 50 µg/L gentamicin at 37 °C under gentle shaking at 90 rpm as described previously (20). After incubation for 3 h tissue slices were collected for the determination of the ATP content, a sensitive marker of the viability of PCLS [6], or for the evaluation of histological integrity using formalin fixed, paraffin-embedded and haematoxylin and eosin stained sections. Incubation of control slices was started directly after slice preparation.

For ATP determination, slices were collected individually in 1 mL 70% ethanol/2 mM EDTA (pH 10.9), snap-frozen in liquid nitrogen and stored at –80 °C until analysis. After thawing, the slices were homogenized for 45 s using a mini bead beater (Biospec Products, USA). After centrifugation at 13,200 rpm for 5 min, the ATP level in the supernatant was determined using the ATP

Bioluminescence assay kit CLS II (Roche diagnostics, Mannheim, Germany) according to the manufacturer's protocol. In brief, the solution was diluted 10 times with 0.1 M Tris HCl containing 2 mM EDTA (pH 7.8). Subsequently, 50  $\mu$ L luciferase solution was added to 50  $\mu$ L sample and the luminescence as a measure of ATP content was measured using a Packard LumiCount<sup>®</sup> Luminescence Microplate Reader (Packard, United Kingdom).

The procedure of haematoxylin and eosin (H&E) staining was as follows. After fixation with 4% formalin at 4 °C for at least 15 h, slices were dehydrated in a graded alcohol series and Histosolve (Thermo Scientific, Pittsburgh, USA). Subsequently, slices from the same experimental group were vertically embedded in paraffin and cross-sectioned at 4- $\mu$ m thickness. The sections were stained with haematoxylin and eosin (H&E). The slice viability was determined by estimating the percentage of viable cells in the slice cross-section. Cells were considered non-viable when they exhibited irreversible changes indicated by eosinophilic cytoplasm, and nuclear changes like pyknosis (condensed nucleus), karyorrhexis (fragmented nucleus) or karyolysis (loss of nucleus).

#### Differential scanning calorimeter measurements

A Perkin Elmer DSC-7 differential scanning calorimeter equipped with a CCA7 cooling device was used to monitor crystallization in the slices during cooling to  $-150$  °C and warming [7]. The CPA solutions themselves do not crystallize during cooling to  $-150$  °C and warming, so if crystallization occurs in the slices this would indicate incomplete penetration of the CPAs. Thermograms of the slices impregnated with CPA were recorded at a cooling rate of 60 °C/min and a warming rate of 5 °C/min from 4 to  $-150$  °C.

#### Statistical methods

All experiments with slices were performed with at least 4 slices for each condition and each liver. Two to five replicates of every experiment were performed. Results are expressed as mean  $\pm$  standard error of the mean (SEM) and significance was tested using a two-tailed, paired Student *t*-test. Results were considered significant when  $p \leq 0.05$ .

## Results

#### Characterization of the newly designed chamber for the gradient method

To test whether the CPA mixed well and the concentration increased according to our calculations, the red dye SRB was added to the CPA that was pumped into the chamber with a flow rate of 1.3 mL/min (Fig. 3). The concentration of the dye was measured at different times during loading of the CPA and compared with the predicted concentrations of the CPA. The results are given in Fig. 6 and indicated immediate mixing of CPA with the buffer solution in the chamber, which allows us to consider the chamber as a well-mixed reactor in our calculations.

As indicated in Fig. 7, exposing slices to a medium flow of 1.3 mL/min for 105 min (which is the maximum time that the slices spent in the chamber with the gradient method) using UW instead of CPAs, did not have an impact on the viability of the liver slices. This was indicated by similar ATP content and morphological integrity compared to slices incubated in static cold UW for the same time.

#### The influence of loading and unloading methods for VM3 on the viability of PCLS

CPA concentration profiles for the various protocols used for loading and unloading of VM3 are shown in Fig. 3.

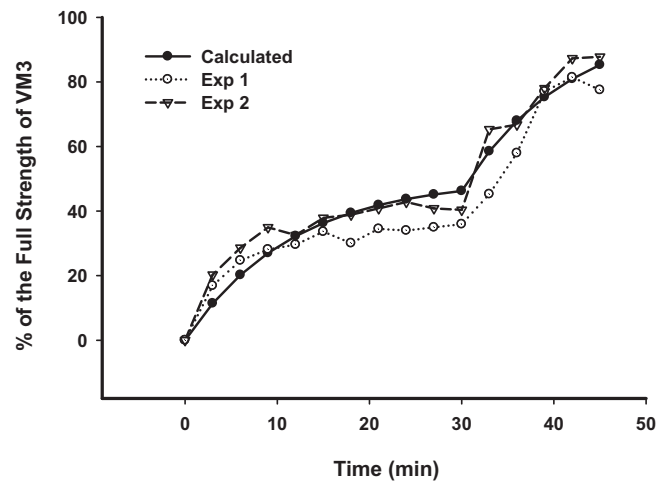


**Fig. 6.** Normalized CPA concentration within the mixing chamber during the CPA loading step. The measured absorbances were normalized to the absorbance induced by 0.18 mg/mL SRB, which is representative for a solution containing 100% VM3. Results of two independent experiments are given as well as the theoretical calculated concentrations. First, 50% VM3 solution containing 0.09 mg/mL SRB was pumped into the chamber at a rate of 1.3 mL/min for 30 min followed by 100% VM3 containing 0.18 mg/mL SRB for 15 min.

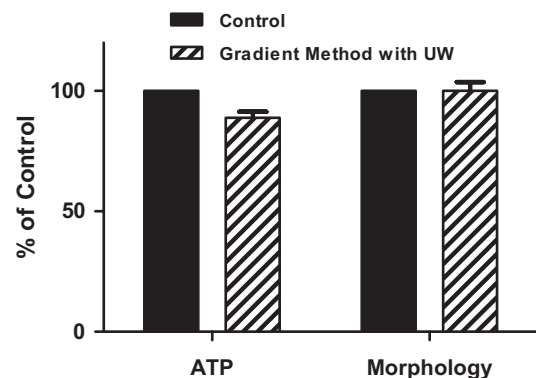


**Fig. 7.** Viability (ATP content and histomorphological scores) of liver slices after exposing the slices to the flow of storage medium (UW) at the maximum flow rate as used during loading of CPA (gradient method with UW), relative to slices that underwent static storage in ice-cold UW medium through the whole procedure (control slices). Histomorphological appearance of slices was quantified as the percentage of intact (not necrotic) cells in the slice cross section. All slices were incubated at 37 °C for 3 h prior to viability testing. Bars indicate the means of three experiments (three slices per experiment)  $\pm$  SEM.

As can be seen from Fig. 8, first a two phase gradient method was applied with a 1.3 mL/min flow rate for VM3 loading and unloading, by first pumping 50% VM3 and after 30 min followed by 100% VM3. This method had an effect on the viability of liver slices that was comparable to the effects of the step-wise method, based on ATP content (about 55% of control slices). Decreasing the flow rate from 1.3 mL/min to 1.0 mL/min resulted in a slight (9%) but not statistically significant ( $p = 0.056$ ) increase of ATP content.

To further study the sensitivity of PCLS to osmotic stress, the rate of concentration change during VM3 loading was increased by pumping 100% VM3 into the chamber without prior perfusion with 50% VMP (one-phase gradient method) (Fig. 3). Afterwards, slices were exposed to 100% VM3 working solution for an additional 15 min. ATP levels using this method were 49% relative to untreated controls and were decreased by 15% compared to the two-phase gradient method but the difference was not statistically significant. (Fig. 8). Moreover, the ATP content of slices directly transferred from 100% VM3 to LM5 for unloading was 3% of control slices.

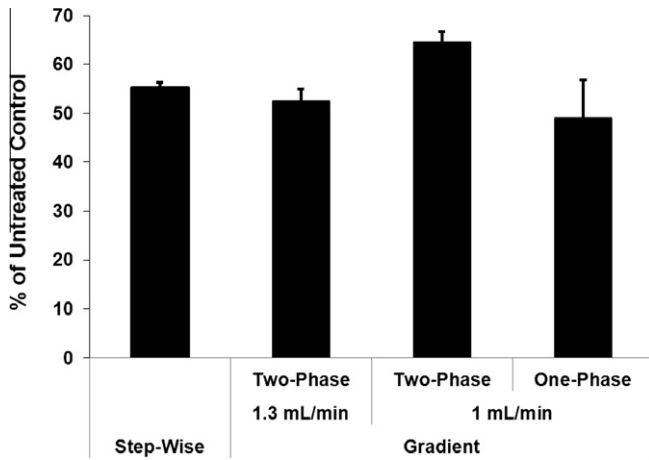


**Fig. 8.** ATP content of liver slices after treatment with VM3 by the step-wise method and the one- and two-phase gradient methods, relative to slices incubated in WME medium directly after slicing. An additional 15 min exposure to 100% VM3 solution was conducted to complete CPA penetration in the PCLS. All slices were incubated at 37 °C for 3 h prior to viability testing. Bars give the means of 2–5 experiments (three slices per experiment) + SEM.

DSC measurements indicated that slices were fully loaded with VM3 by all protocols as no ice crystals were formed during cooling and warming of loaded slices (data not shown).

*The influence of loading and unloading methods for M22 on the viability of PCLS*

The gradient protocol developed for VM3 was applied to M22 loading/unloading. Although the concentration changes were much steeper (Fig. 4) and the total exposure time to 100% M22 was much longer in the step-wise method than in the gradient method (19 vs 5 min), the viability of liver slices after exposure to M22 using the gradient methods followed by 5 min additional impregnation with 100% M22 was comparable (70%) to that of slices that were exposed to M22 using the step-wise method (Fig. 9). Prolonging the additional incubation time in 100% M22 working solution to 15 min decreased the ATP content in the liver slices, but this decrease was not statistically significant. The ATP content of slices incubated for 15 additional min with 100% M22 after loading with the stepwise method was significantly lower than of slices loaded with the gradient method ( $p < 0.01$ ). Although the total exposure time to M22 was the same with both methods, the exposure time to 100% M22 was much longer with the stepwise method, which may explain the observed differences in viability.

DSC measurement showed that 5 min of additional impregnation with 100% M22 working solution was sufficient to prevent ice crystal formation during cooling and warming, indicating that the slices reached sufficient equilibrium with M22.

*The influence of loading and unloading methods for mM22 on the viability of PCLS*

mM22 was introduced to the slices according to the different protocols as described in Fig. 5. mM22 is somewhat less concentrated than M22 (it contains less methylformamide), but it did not improve the viability of liver slices compared with M22. Even comparing the gradient method for mM22 to the stepwise method for M22, for which the exposure time to M22 was greater than the exposure time for mM22 in the gradient method, there was still no improvement with mM22. As was the case with M22, the ATP levels of slices after mM22 treatment with the gradient methods declined when the additional incubation time with 100% working solution CPA was increased from 5 to 15 min (Fig. 10). In addition,

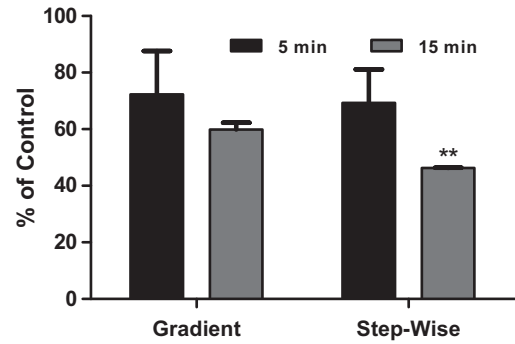


**Fig. 9.** ATP content of liver slices after treatment with M22 by the step-wise and gradient method, relative to slices incubated in WME media directly after slicing. All slices were incubated at 37 °C for 3 h prior to viability testing. After loading within the chamber, slices were incubated in 100% CPA for an additional 5 or 15 min. Bars represent the means of three experiments (three slices per experiment) + SEM. \*\*Values are significantly lower than those of slices that were treated using the gradient method ( $p < 0.01$ ).

as was true for M22, DSC results indicated that after 5 min incubation, slices were sufficiently loaded with mM22 to escape ice formation during cooling and warming.

Unfortunately, the viability of liver slices was not improved by using mM22 diluted to 80% of full strength (0.8× mM22) as indicated by ATP levels, but the stability of the slices against ice formation was compromised by this dilution, and devitrification was observed in the slices upon warming (data not shown).

**Discussion**

We developed a CPA loading/unloading method that gradually introduces CPA solutions into an equilibration chamber containing precision-cut tissue slices, thereby steadily increasing their concentrations, with the aim of reducing osmotic stress. Likewise, during CPA unloading abrupt changes in concentration are prevented using this method.

With the gradient method, the CPA solution is introduced at a constant rate via an inlet into the chamber and at the same time, the medium within the chamber is eliminated via the outlet. Our dye study indicated that to a good approximation, immediate mixing of infused CPA with the chamber constituents occurred, which allowed us to calculate and to control the CPA concentration to which PCLS were exposed as a function of time.

In simpler cell systems, mathematical simulations can be performed to optimize step-wise CPA loading and unloading and minimize osmotic damage [9,24], and microfluidic devices

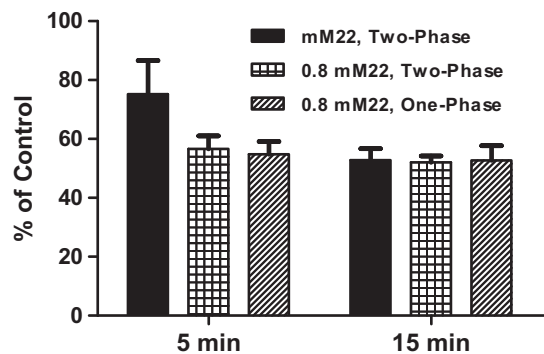


**Fig. 10.** ATP content of liver slices after treatment with full-strength or 80% mM22 by different gradient methods relative to slices incubated in WME media directly after slicing. Additional 5 or 15 min impregnation in 100% mM22 was conducted to complete CPA penetration in the PCLS. All slices were incubated at 37 °C for 3 h prior to viability testing. Bars give the means of 2–5 experiments (three slices per experiment) + SEM.

[16,19,31] can be used to introduce CPA gradually. Such systems allow following volume changes in single cells in response to CPA concentration changes, from which membrane permeability to a single cryoprotectant and to water can be measured. Similar but more empirical studies have been done on tissue slices, yielding shrink-swell curves from which time constants can be calculated from curve fits to the data to yield phenomenological indices of equilibration rates. These equilibration rates can be used to establish protocols for addition and washout of cryoprotectants similar to the way more formal determinations of membrane permeability and hydraulic conductivity are performed [11,34]. Radioactive tracers can also be used to follow the time course of permeation of individual cryoprotectants into and out of tissue slices [3]. However, these methods have various drawbacks, such as the tendency to lose tissue on blotting in gravimetric methods and neither of these methods addresses the heterogeneity of the tissue [4]. The liver contains several cell types, including hepatocytes, Kupffer cells, stellate cells, biliary epithelial cells, endothelial cells, and other cell types, and global osmotic responses may not reflect the properties and the requirements of these individual cell populations. Moreover, in the present study the CPA solutions used were a mixture of up to five nominally permeating CPAs and up to three different impermeable polymers (ice-blockers and PVP), making precise modeling difficult. Since our aim is to develop methods that preserve maximum viability, we elected at this stage to use viability as the endpoint of our study, for which the conventional trial and error method is adequate.

Optimization of CPA loading/unloading in a step-wise protocol is somewhat tedious and time consuming. In contrast, the gradient method described in this paper is more time and cost-effective. It does not require the preparation of a graded series of CPA solutions, but only LM5 and one full-strength CPA solution are needed for CPA loading and LM5 with impermeable sugar for CPA unloading. Furthermore, the process is automated and does not require constant monitoring once the program for the pump is set up, which might in turn reduce inter-experimental and operator-dependent variation and facilitate the standardization of the CPA loading/unloading protocol. Once optimized, this gradient method can be universally used to efficiently evaluate different CPA solutions.

One of the parameters that may influence slice viability is the flow rate for CPA delivery to the PCLS. High flow rate on the one hand might reduce the exposure time of PCLS to CPA which in turn potentially decreases the damage by chemical toxicity, but on the other hand high flow rate and faster concentration changes might damage PCLS due to shear stress and osmotic stress respectively. The optimum flow rate is, however, easy to determine. For the time being, we have not observed a difference between 1 and 1.3 ml/min in terms of their effects on the viability of the PCLS.

Since we eventually aim to successfully vitrify slices after CPA introduction, it is critical that the selected protocols enable sufficient equilibration of the slices with the CPAs to prevent ice crystal formation during cooling and rewarming while at the same time restricting the total exposure time to a minimum to reduce chemical toxicity. As we showed that 80% mM22 is not sufficient to prevent ice-crystal formation, most PCLS were exposed to 100% working solutions after the gradient protocol. The results indicated that 5 min additional exposure to M22 and mM22 was sufficient to prevent crystallization during cooling and warming, which implies rapid osmotic equilibration between the slices and their surrounding medium. At the end of the CPA loading and unloading procedure, slices were incubated with LM5 with 300 mM trehalose for another 15 min to complete unloading of the CPA, which is critical, because these compounds at 37 °C can be toxic even at very low concentrations [18,33].

With the designed semi-automated gradient method, we expected better viability of PCLS to be achieved since the gradual

changes of CPA avoided rapid and large changes in osmolarity as imposed in the step-wise method and thereby was expected to minimize osmotic stress. However, although there were hints of osmotic effects in some experiments, we observed that the viability of PCLS after using the gradient method was in most cases comparable to that of the step-wise method. Also, reducing the flow rate or increasing the infused CPA concentration did not affect the viability of the slices. A likely explanation for our observations is that the step-wise protocols used for M22 and VM3 were already well optimized and apparently did not introduce any significant osmotic damage. Although liver slices appear tolerant of large osmotic gradients, direct transfer of the PCLS from 100% working solution CPA into LM5 in one step completely deteriorated the slices (ATP content of the slice was then 3% of control), so it is clear that osmotic stress can cause damage if it exceeds certain limits.

It is also possible that subtle damage from osmotic stress might only be observed after extra stress from other sources, such as chemical toxicity from longer exposure or chilling injury during vitrification. Song [31] also found that gradual loading and unloading of CPAs only provided a higher viability outcome after extra stress, i.e. freezing. Possibly more sensitive parameters to indicate osmotic stress such as altered regulation of a specific set of genes suggested to be involved in the reaction to osmotic stress ([http://www.sabiosciences.com/rt\\_pcr\\_product/HTML/PARN-151A.html](http://www.sabiosciences.com/rt_pcr_product/HTML/PARN-151A.html)), as an early marker, would give more insight into the osmotic stress induced by CPAs.

Since the viability of the slices could not be clearly improved despite the reduction of osmotic stress and remained considerably lower than that of untreated slices, we conclude that the chemical toxicity of the CPAs still remains the main barrier to overcome. Among all the CPAs tested, M22 is the most concentrated but the least toxic as indicated by the ATP level, even when exposure to it is prolonged. mM22, less concentrated than M22, was not less toxic, and reducing its concentration to just 80% of full strength did not reduce its toxicity. Therefore, the amount of injury observed was not proportional to osmotic stress but, it was also not proportional to the total amount of CPA present in the solutions, nor was it strongly dependent on exposure time at the highest concentrations, all of which would normally be expected to correlate with injury even when osmotic damage is excluded. This peculiar finding suggests that the injury in this case may relate largely to the presence of one or several components in all of the solutions, rather than to osmotic stress.

## Conclusion

In the present study we developed a semi-automated method for gradual loading and subsequent unloading of CPA in tissue slices. The gradient method for CPA loading and unloading ensured sufficient CPA penetration into the slices to render them stable against ice formation after vitrification and rewarming at only 5 °C/min, and appeared much more efficient and less labor intensive than the usual step-wise method. However, compared with the step-wise method, the gradient method could not improve the viability of PCLS, although rates of change in osmolarity were greatly reduced. For liver slices, chemical toxicity of as yet unidentified components of the CPA solutions remains the main barrier to be overcome.

## References

- [1] B. Burkhardt, J. Wittenauer, E. Pfeiffer, U.M. Schauer, M. Metzler, Oxidative metabolism of the mycotoxins alternariol and alternariol-9-methyl ether in precision-cut rat liver slices in vitro, *Mol. Nutr. Food Res.* 55 (2011) 1079–1086.
- [2] P. Carranza-Rosales, M.G. Santiago-Mauricio, N.E. Guzman-Delgado, J. Vargas-Villarreal, G. Lozano-Garza, J. Ventura-Juarez, I. Balderas-Renteria, J. Moran-Martinez, A.J. Gandolfi, Precision-cut hamster liver slices as an ex vivo model to study amoebic liver abscess, *Exp. Parasitol.* 126 (2010) 117–125.

- [3] P. Clark, G.M. Fahy, A.M. Karow Jr., Factors influencing renal cryopreservation. I. Effects of three vehicle solutions and the permeation kinetics of three cryoprotectants assessed with rabbit cortical slices, *Cryobiology* 21 (1984) 260–273.
- [4] Z.F. Cui, R.C. Dykhuizen, R.M. Nerem, A. Sembanis, Modeling of cryopreservation of engineered tissues with one-dimensional geometry, *Biotechnol. Prog.* 18 (2002) 354–361.
- [5] I.A. de Graaf, A.L. Draaisma, O. Schoeman, G.M. Fahy, G.M. Groothuis, H.J. Koster, Cryopreservation of rat precision-cut liver and kidney slices by rapid freezing and vitrification, *Cryobiology* 54 (2007) 1–12.
- [6] I.A. de Graaf, H.J. Koster, Cryopreservation of precision-cut tissue slices for application in drug metabolism research, *Toxicol. In Vitro* 17 (2003) 1–17.
- [7] I.A. de Graaf, P. Olinga, M.H. de Jager, M.T. Merema, R. de Kanter, E.G. van de Kerkhof, G.M. Groothuis, Preparation and incubation of precision-cut liver and intestinal slices for application in drug metabolism and toxicity studies, *Nat. Protoc.* 5 (2010) 1540–1551.
- [8] U. Demirci, G. Montesano, Cell encapsulating droplet vitrification, *Lab Chip* 7 (2007) 1428–1433.
- [9] W. Ding, X. Zhou, S. Heimfeld, J.A. Reems, D. Gao, A steady-state mass transfer model of removing CPAs from cryopreserved blood with hollow fiber modules, *J. Biomech. Eng.* 132 (2010) 011002.
- [10] G.M. Fahy, Cryoprotectant toxicity neutralization, *Cryobiology* 60 (2010) S45–S53.
- [11] G.M. Fahy, Cryoprotectant toxicity: biochemical or osmotic?, *Cryo Lett.* 5 (1984) 79–90.
- [12] G.M. Fahy, D.R. MacFarlane, C.A. Angell, H.T. Meryman, Vitrification as an approach to cryopreservation, *Cryobiology* 21 (1984) 407–426.
- [13] G.M. Fahy, B. Wowk, R. Pagotan, A. Chang, J. Phan, B. Thomson, L. Phan, Physical and biological aspects of renal vitrification, *Organogenesis* 5 (2009) 167–175.
- [14] G.M. Fahy, B. Wowk, J. Wu, S. Paynter, Improved vitrification solutions based on the predictability of vitrification solution toxicity, *Cryobiology* 48 (2004) 22–35.
- [15] G.M. Fahy, B. Wowk, J. Wu, J. Phan, C. Rasch, A. Chang, E. Zendejas, Cryopreservation of organs by vitrification: perspectives and recent advances, *Cryobiology* 48 (2004) 157–178.
- [16] K.K. Fleming Glass, E.K. Longmire, A. Hubel, Optimization of a microfluidic device for diffusion-based extraction of dmsol from a cell suspension, *Int. J. Heat Mass Transfer* 51 (2008) 5749–5757.
- [17] B.J. Fuller, Cryoprotectants: the essential antifreezes to protect life in the frozen state, *Cryo. Lett.* 25 (2004) 375–388.
- [18] A.M. Hak, F.G. Offerijns, C.C. Verheul, Toxic effects of DMSO on cultured beating heart cells at temperatures above zero, *Cryobiology* 10 (1973) 244–250.
- [19] Y.S. Heo, H.J. Lee, B.A. Hassell, D. Irimia, T.L. Toth, H. Elmoazzen, M. Toner, Controlled loading of cryoprotectants (CPAs) to oocyte with linear and complex CPA profiles on a microfluidic platform, *Lab Chip* 11 (2011) 3530–3537.
- [20] K.I. I. Vladimir, I. Evgenia, in: M.J. Tucker, J. Liebermann, (Eds.), in *Vitrification in Assisted Reproduction: A User's Manual and Trouble-shooting Guide*, Infarma Healthcare Medical Books, Oxon, 2007, pp. 21–32.
- [21] H.U. Kasper, E. Konze, N. Kutinova Canova, H.P. Dienes, V. Dries, Cryopreservation of precision cut tissue slices (PCTS): investigation of morphology and reactivity, *Exp. Toxicol. Pathol.* 63 (2011) 575–580.
- [22] W.J. Maas, I.A. de Graaf, E.D. Schoen, H.J. Koster, J.J. van de Sandt, J.P. Groten, Assessment of some critical factors in the freezing technique for the cryopreservation of precision-cut rat liver slices, *Cryobiology* 40 (2000) 250–263.
- [23] F. Migishima, R. Suzuki-Migishima, S.Y. Song, T. Kuramochi, S. Azuma, M. Nishijima, M. Yokoyama, Successful cryopreservation of mouse ovaries by vitrification, *Biol. Reprod.* 68 (2003) 881–887.
- [24] I.N. Mukherjee, Y.C. Song, A. Sambanis, Cryoprotectant delivery and removal from murine insulinomas at vitrification-relevant concentrations, *Cryobiology* 55 (2007) 10–18.
- [25] C.G. Paniagua-Chavez, T.R. Tiersch, Laboratory studies of cryopreservation of sperm and trochophore larvae of the eastern oyster, *Cryobiology* 43 (2001) 211–223.
- [26] D.E. Pegg, M.P. Diaper, in: C.T. Smit Sibinga, P.C. Das, H.T. Meryman (Eds.), *In Cryopreservation and Low Temperature Biology in Blood Transfusion*, Kluwer Academic Publishers, Dordrecht, 1990, pp. 55–69.
- [27] Y. Pichugin, G.M. Fahy, R. Morin, Cryopreservation of rat hippocampal slices by vitrification, *Cryobiology* 52 (2006) 228–240.
- [28] A.B. Renwick, P.S. Watts, R.J. Edwards, P.T. Barton, I. Guyonnet, R.J. Price, J.M. Tredger, O. Pelkonen, A.R. Boobis, B.G. Lake, Differential maintenance of cytochrome P450 enzymes in cultured precision-cut human liver slices, *Drug Metab. Dispos.* 28 (2000) 1202–1209.
- [29] E. Richter, S. Friesenegger, J. Engl, A.R. Tricker, Use of precision-cut tissue slices in organ culture to study metabolism of 4-(methylnitrosamino)-1-(3-pyridyl)-1-butanol (NNK) and 4-(methylnitrosamino)-1-(3-pyridyl)-1-butanol (NNAL) by hamster lung, liver and kidney, *Toxicology* 144 (2000) 83–91.
- [30] M. Sato, K. Yokokawa, K. Kasai, N. Tada, Successful vitrification of stroke-prone spontaneously hypertensive and normal Wistar rat 2-cell embryos, *Lab Anim.* 30 (1996) 132–137.
- [31] Y.S. Song, S. Moon, L. Hulli, S.K. Hasan, E. Kayaalp, U. Demirci, Microfluidics for cryopreservation, *Lab Chip* 9 (2009) 1874–1881.
- [32] S. Sreelatha, P.R. Padma, Protective mechanisms of *Moringa oleifera* against CCl<sub>4</sub>-induced oxidative stress in precision-cut liver slices, *Forsch. Komplementmed* 17 (2010) 189–194.
- [33] E.A. Szurek, A. Eroglu, Comparison and avoidance of toxicity of penetrating cryoprotectants, *PLoS One* 6 (2011) e27604.
- [34] L.I. Tsonev, K.N. Stoiancheva, G.M. Fahy, Permeation of 2,3-butanediol and dimethyl sulfoxide in renal cortex, *Cryo. Lett.* 15 (1994) 251–266.
- [35] M. Van de Bovenkamp, G.M. Groothuis, D.K. Meijer, P. Olinga, Liver fibrosis in vitro: cell culture models and precision-cut liver slices, *Toxicol. In Vitro* 21 (2007) 545–557.
- [36] M. van de Bovenkamp, G.M. Groothuis, D.K. Meijer, P. Olinga, Precision-cut fibrotic rat liver slices as a new model to test the effects of anti-fibrotic drugs in vitro, *J. Hepatol.* 45 (2006) 696–703.
- [37] M.C. Wusteman, J. Simmonds, D. Vaughan, D.E. Pegg, Vitrification of rabbit tissues with propylene glycol and trehalose, *Cryobiology* 56 (2008) 62–71.
- [38] J. Zhang, J. Cui, X. Ling, X. Li, Y. Peng, X. Guo, B.C. Heng, G.Q. Tong, Vitrification of mouse embryos at 2-cell, 4-cell and 8-cell stages by cryotop method, *J. Assist. Reprod. Genet.* 26 (2009) 621–628.